

DEVELOPMENT OF A CONCEPTUAL DESIGN TOOL FOR VARIOUS COMPOUND HELICOPTERS

Donguk Lee¹, Soomin Jeong¹, Kwanjung Yee^{2*}

¹Dept. of mechanical and Aerospace Engineering
Seoul National University, Seoul, 08826, Republic of Korea
oak600p@snu.ac.kr / sminjeong@snu.ac.kr

²Institute of Advanced Aerospace Technology
Seoul National University, Seoul, 08826, Republic of Korea
kjyee@snu.ac.kr

ABSTRACT

Recent rotorcraft community has suggested various forms of compound helicopters capable of carrying out a high-speed maneuver. These aircraft have disparate aerodynamic characteristics and propulsion system due to their unique way of generating lift and thrust. In view of the unique features, each concept is adapted with a specific mission profile. To provide an appropriate concept for a specific mission, this study developed a comprehensive conceptual design tool for the three concepts, winged helicopter, tip-jet gyroplane, and fan-in-body concept. This design tool enables sizing of the compound helicopters with comparable analysis fidelity, while considering their distinctive propulsion system at the conceptual design phase. With the developed tool, the design optimizations were conducted for six different mission profiles covering various flight range, hover and loiter time. Subsequently, systematic comparisons and analyses were carried out to deduce the most appropriate configuration for each mission.

NOMENCLATURE AND ABBREVIATIONS

A	= Disk area (ft ²)	K	= Loss coefficient
AR	= Aspect ratio	L	= Lift Force (lb)
a_0	= Rotor coning angle (rad)	LS	= Lift sharing factor (lb)
a_1, b_1	= Coefficient of $\cos\psi$ for β	$l_{a.c}$	= Non-dimension length from root chord and aerodynamic center
$BEMT$	= Blade element momentum theory	$l_{c.g}$	= Non-dimension length from root chord and center of gravity
BET	= Blade element theory	l_{fuse}	= Fuselage length (ft)
b	= Span (ft)	l_h	= Length between main wing and tail wing (ft)
C_D	= Drag coefficient (3-D)	l_n	= Non-dimension length from root chord to neutral point
C_{d0}	= Drag coefficient (2-D)	M	= Mach number
C_L	= Lift coefficient (3-D)	M_{dd}	= Drag divergence Mach number
$C_{L\alpha}$	= Slope of lift curve (3-D)	MT	= Momentum theory
$C_{L\alpha,WB}$	= Slope of lift curve without the wing-body interference(3-D)	N	= Number
$C_{l\alpha}$	= Slope of lift curve (2-D)	P	= Power (HP)
C_T	= Thrust coefficient	P_{avail}	= Available power (HP)
c	= Chord (ft)	P_{co}	= Coriolis power (HP)
\bar{c}	= Mean chord length (ft)	P_i	= Induced power (HP)
D	= Drag force (lb)	P_{max}	= Maximum power (HP)
d	= Diameter (ft)	P_t	= Total Pressure (lb/ft ²)
e	= Span efficiency factor	P_0	= Induced power (HP)
F	= Force (lb)	PR	= Pressure ratio
F_p	= Prandtl's function	Q	= Torque (lb-ft)
FIB	= Fan-in-body	q_∞	= Dynamic pressure (lb/ft ²)
f	= Friction coefficient	R	= Radius (ft)
f_e	= Equivalent flat plate area (ft ²)	R_{gas}	= Gas constant (lb-ft/(slug·°R))
H	= Horizontal force (lb)	R_{tip}	= Rip radius (ft)
HT	= Horizontal tail	Re	= Reynold's number
h	= Height (ft)	S	= Wing area (ft ²)
SR	= Slow down ratio of the main rotor	ε	= Surface roughness (ft)
T	= Thrust (lb)	ζ	= Transmission loss ratio
TR	= Thrust ratio (T_{prop}/T_{total})	\dot{m}	= Mass flow (lb/s)

$TOGW$	= Take-off gross weight (lb)	θ_{tw}	= Twist angle (rad)
T_{exit}	= Static temperature at the compressor exit (°R)	θ_i	= Incidence angle (rad)
t	= Thickness (ft)	θ_0	= Collective pitch angle (rad)
V	= Volume (ft ³)	κ	= Induced power factor
VT	= Vertical tail	κ_{type}	= Rotor weight factor
V_∞	= Free stream velocity (ft/s)	Λ	= Sweepback angle of c/4 line(deg)
V_{jet}	= Jet Velocity (ft/s)	λ	= Taper ratio
V_{tip}	= Velocity at the rotor tip (ft/s)	λ_c	= Climbing velocity ratio
v_i	= Induced velocity (ft/s)	λ_i	= Induced velocity ratio
W	= Component weight (lb)	λ_{total}	= Inflow velocity ratio
w_i	= Slip stream velocity (ft/s)	μ	= Advance ratio
W_{press}	= Weight penalty due to pressurization	ρ	= Density (slug/ft ³)
α	= Angle of attack (rad)	ρ_0	= Air density (slug/ft ³)
α_{eff}	= Effective angle of attack (rad)	σ	= Solidity
α_{tilt}	= Shaft tilt angle (rad)	σ_d	= Expansion ratio
β	= Flapping angle at particular azimuth angle	ν	= Flap natural frequency (per rev)
γ	= Ratio of specific heats	χ	= Wake skew angle
γ_{lock}	= Lock number	ψ	= Blade azimuth angle
δ	= Tip clearance (ft)	$\frac{\partial \epsilon}{\partial \alpha}$	= Rate of change of tail downwash
Subscript			
b	= Blade	TPP	= Tip path plane
eng	= Engine	t	= Horizontal tail wing
$fuse$	= Fuselage	w	= Main Wing
N	= Nozzle	$xmsn$	= Transmission
$prop$	= Auxiliary propeller	v	= Vertical (Z-direction)
r	= Rotor		

1. INTRODUCTION

Helicopters are classified as runway independent aircraft and are capable of adapting to various environment. However, it is limited by the dynamic stall, lift imbalance, and vibrations generated at the rotor during high-speed maneuver. Such limitations have restricted these aircraft to have 150–180 knot maximum flight speed, and cruising speed of 130–150knots [1]. High speed flight is desirable especially for reconnaissance mission that requires flexible and agile combat capabilities. As such, VTOL and high-speed maneuver capable helicopters are required. To this end, combination of fixed-wing aircraft's high-speed maneuver and rotorcraft's VTOL capability have led to the invention of the compound helicopter. Various concepts for compound helicopter have been suggested which possess different aerodynamic characteristics and propulsion system according to the configurations.

To begin with, Eurocopter has been developing the winged helicopter concept known as the X3. Winged helicopter differs from the conventional helicopter by having a wing and an auxiliary thrust device aside from the main rotor. This configuration enables a high speed maneuver by providing the additional lift and thrust by the mechanism such as the wing and the auxiliary thrust device. Another form of compound helicopter is DARPA have led the tip-jet gyroplane concept as part of the Heliplane Program. Tip-jet Gyroplane is a compound helicopter with tip-driven rotor, the auxiliary propeller and the wing. Equipped with the tip-driven rotor, it is unnecessary to have the transmission installed. Since it flies in a form of a gyroplane, a greater portion of engine power can be used for the high-speed maneuver. Additionally, Boeing has been conducting the fan-in-body

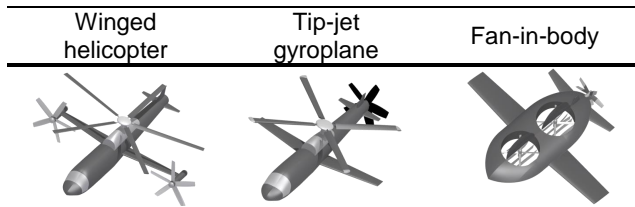
concept as part of the VTOL X-plane program. Fan-in-body concept is considered a compound helicopter that combines ducted fan and wing. This concept uses the ducted fan to perform hover and axial flight, and flies like a fixed-wing aircraft during forward flight. Without the rotor restricting the aircraft, it is capable to perform a high speed maneuver.

To design various compound helicopter concepts, novel analysis and design method are required. Roche[2] carried out and compared winged helicopter with conventional helicopter. Vu[3] developed the conceptual design tool and carried out optimizations for the tip-jet gyroplane. Lee[4] proposed a new aerodynamic analysis method for conceptual design of a lift fan aircraft. However, these studies were only limited to analyze a specific concept of a compound helicopter. Because of their unique feature, each concept is suited with a specific mission profile. For comprehensive analysis to be carried out, it is important to design the compound helicopters at the same fidelity and analyse their characteristic by comparing with their performance. Therefore, this study developed a comprehensive conceptual design tool for the three concepts, winged helicopter, tip-jet gyroplane, and fan-in-body concept as shown in Table 1. This design tool allows sizing of the three compound helicopter with comparable analysis fidelity level, considering their distinctive propulsion system at the conceptual design phase. Rotor aerodynamic analysis was based on the blade element momentum theory (BEMT) and the blade element theory (BET). Propeller analysis was carried out using the momentum theory(MT). In addition, wing aerodynamic analysis was based on the Oswald's factor to consider the 3D effects of the wing. Since the proposed three concepts have distinct variation in flight performance, mission

analysis for each concept is configured accordingly.

In this study, design optimizations of compound helicopters performing six various mission profiles were carried out. Through the optimization, appropriate concepts were suggested for various flight range, hover and loiter time.

Table 1: Types of Compound Helicopters



2. CONCEPTUAL DESIGN METHOD

2.1. Overall Design Flow

Compound helicopter design framework was further developed based on the preliminary design methodology study [5]. Mission analyses for various concepts are incorporated accordingly, and the overall framework design flowchart is shown in Fig 1. Through 1) ~ 7) procedures, compound helicopter design was conducted. 1) Inputs (variables and design parameters) are used to calculate geometries (disk area, solidity, etc.) of the helicopter. 2) Using the initial TOGW and the lift sharing factor, wing sizing capable of carrying out the mission is carried out. Then, the wing position that satisfies the static margin of the design parameter is determined using the equation (A1). 3) Engine sizing is carried out based on the rubber engine methodology introduced in the SSP program [6]. 4) Empty weight, using the weight estimation formula at the appendix, is calculated. 5) Fuel weight required to carry out the mission is calculated within the mission analysis module. 6) Using the calculated empty weight and the fuel weight, the payload is obtained. An iterative calculation is performed, correcting the TOGW until the calculated empty weight is within 3% error with the targeted payload. 7) Until the termination condition is met, design variables are manipulated to obtain an optimized result. Since the proposed three concepts have distinct variation in flight performance, mission analysis for each concept is configured accordingly, and detailed explanations are described in section 2.2~2.4.

2.2. Mission Analysis : Winged Helicopter

Winged helicopter differs from the conventional helicopter by having a wing and an auxiliary thrust device aside from the main rotor. The flight performance of the winged helicopter is shown in Table 2. While hovering, torque generated by the main rotor is counteracted by the auxiliary propeller as depicted in Figure 2. During forward flight, the main rotor and the wing produce lift, and the main rotor and the propeller generate thrust.

Table 2: Flight Performance of Winged Helicopter

	Flight condition	Force generation
Winged helicopter	Hover, Axial	Rotor, Prop
	Cruise	Rotor, Wing, Prop

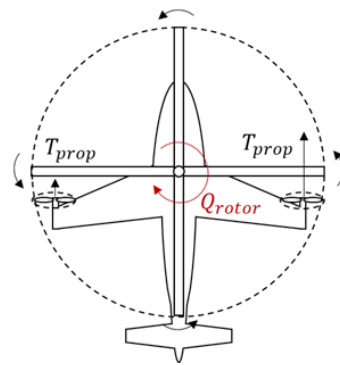


Figure 1: Acting Forces at Hovering (Winged)

2.2.1. Hovering, Axial Flight Analysis

Through steps 1) ~ 4), hover and axial flight analysis module calculates the required power as shown in the Fig 3 flowchart. 1) Using the equation (1) on BEMT, the rotor analysis is performed using the input gross weight and the geometry parameters [7]. 2) Utilizing the equation (2), additional vertical drag of the fuselage and the wing generated by the rotor wake is calculated [8]. 3) Using the equation (3), auxiliary propeller analysis, based on the MT, is performed to cancel the torque generated by the rotor [7]. 4) Assuming a fixed transmission loss, the required power is calculated for both hover and axial flight mission.

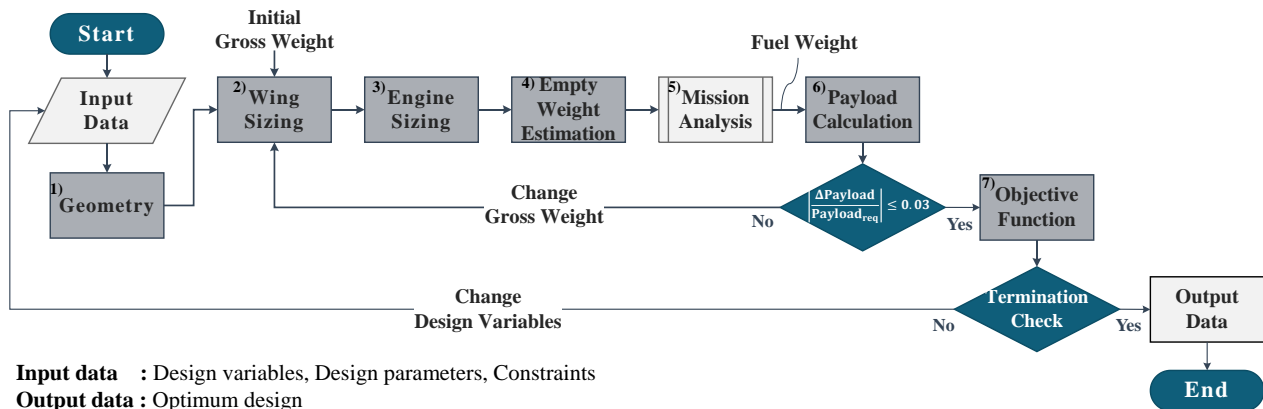


Figure 2: Overall Design Flow Chart

$$(1) C_T = \sum_{n=1}^N \left[\frac{\sigma C_{l\alpha}}{2} (\theta(r_n)r_n^2 - \lambda_{total}(r_n)r_n) \Delta r \right]$$

$$\lambda_{total}(r, \lambda_c) = \sqrt{\left(\frac{\sigma C_{l\alpha}}{16F_p} - \frac{\lambda_c}{2} \right)^2 + \frac{\sigma C_{l\alpha}}{8F_p} \theta r} - \left(\frac{\sigma C_{l\alpha}}{16F_p} - \frac{\lambda_c}{2} \right)$$

$$(2) T = GW + D_v, \quad D_v = \frac{1}{2} \rho_0 f_{ev} w_i^2$$

$$(3) v_{i,prop} = \sqrt{\frac{T_{prop}}{2\rho_0 A}}, \quad T_{prop} = \frac{Q_r}{0.5b_w}$$

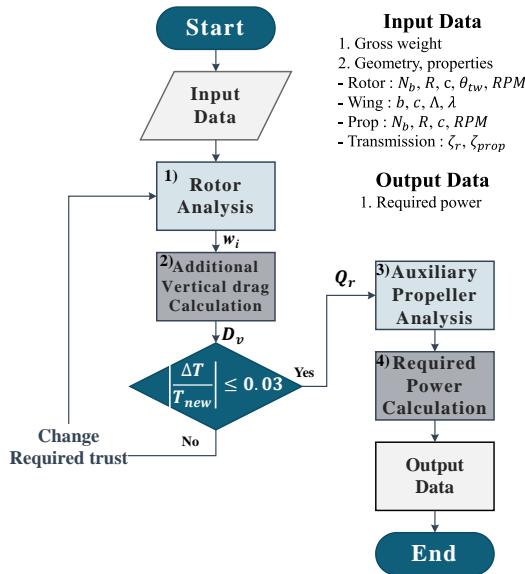


Figure 3: Hovering, Axial Flight Analysis Flow Chart (Winged)

2.2.2. Cruise Analysis (Winged)

Cruise analysis for the winged helicopter is depicted in Fig 4, calculating the required power, fuselage angle and the lift sharing factor through 1) ~ 6) processes. 1) The wing analysis is performed with the input gross weight and geometry shape parameters. Using the Oswald factor in equation (4), the wing analysis considers for the three-dimensional effects of the wing [9]. The lift sharing factor is then derived from the calculated lift as shown in equation (5). 2) Using the BET, analysis of the main rotor producing lift equivalent to the derived lift sharing factor is carried out. With linear twist assumption of the rotor and the uniform inflow model, the collective pitch angle and the flapping motion are derived from equation (6) and (7) [10]. 3) Utilizing the equation (9), additional vertical drag of the fuselage and the wing generated by the rotor wake is calculated with the slip stream velocity and the wake skew angle [2]. 4) With equation (10), auxiliary propeller, producing thrust equivalent to k_{prop} portion of total drag, is analyzed using the MT. 5) The fuselage angle that balances all the forces acting on the aircraft in Fig. 5 is iteratively calculated. 6) Assuming a fixed transmission loss, the required power is calculated for the cruise mission.

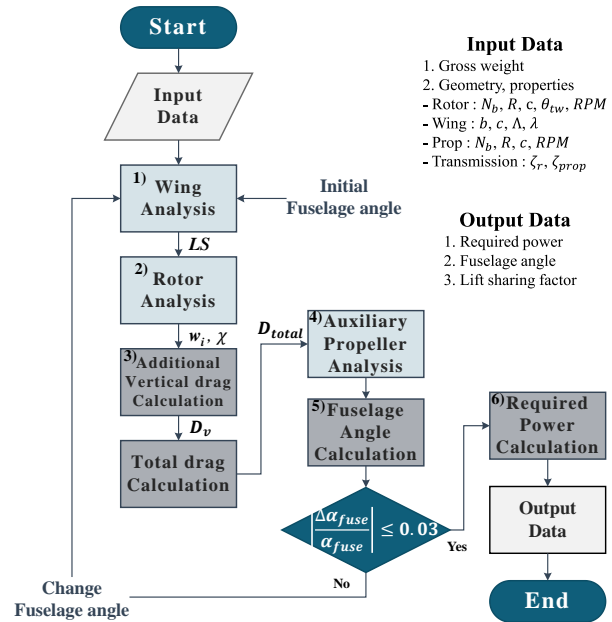


Figure 4: Cruise Analysis Flow Chart (Winged)

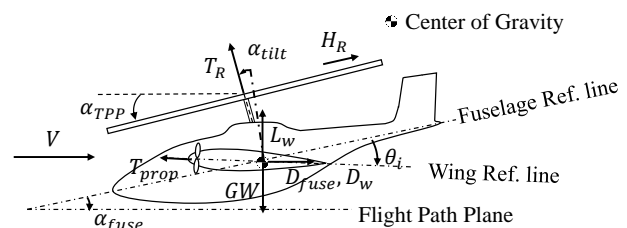


Figure 5: Acting Force at Cruise (Winged)

$$(4) C_{L\alpha} = \frac{C_{l\alpha}}{1 + \frac{C_{l\alpha}}{ARe}}, \quad C_D = C_{d0} + \frac{C_L^2}{\pi ARe}$$

$$(5) LS = 1 - \frac{L_w}{GW}$$

$$(6) \lambda_{TPP} = \mu \tan(\alpha_{TPP}) + \frac{C_T}{2\sqrt{\mu^2 + \lambda_{TPP}^2}}$$

$$(7) \theta_0 = \frac{3}{1 + 1.5\mu^2} \left[\frac{2C_T}{\sigma C_{l\alpha}} - \frac{\lambda_i}{2} - \frac{\theta_{tw}}{4} (1 + \mu^2) \right]$$

$$(8) \beta = a_0 + a_1 \cos(\psi) + b_1 \sin(\psi)$$

$$a_0 = \frac{1}{2} \gamma_{lock} \left[\frac{\theta_0}{4} (1 + \mu^2) + \frac{\theta_{tw}}{30} (6 + 5\mu^2) - \frac{\lambda_i}{3} \right]$$

$$a_1 = - \frac{\mu \left(\frac{8}{3} \theta_0 + 2\theta_{tw} - 2\lambda_i \right)}{1 - \frac{\mu^2}{2}}$$

$$b_1 = - \frac{4\mu a_0}{3 \left(1 + \frac{\mu^2}{2} \right)}$$

$$(9) D_v = \frac{1}{2} \rho_0 f_{ev} w_i^2 \cos(\chi)$$

$$(10) F_{x,prop} = k_{prop} (D_{fuse} + D_w + H_R \cos(\alpha_{TPP}))$$

2.3. Mission Analysis : Tip-Jet Gyroplane

Tip-jet gyroplane is a compound helicopter with tip-driven rotor, the auxiliary propeller and the wing. During hover, axial flight, the main rotor is rotated by the variable nozzle expelling jet at the rotor blade tip. During forward flight, tip-jet gyroplane flies in a form of a gyroplane [3]. For this configuration, the tip-path-plane angle and the rotating speed of the rotor are adjusted by tilting the rotor shaft axis. During the transition flight, all combination of the tip-jet system, the wing, and the auxiliary propeller are used to generate the lift and the thrust.

Table 3: Flight Performance of Tip-Jet Gyroplane

	Flight condition	Force generation
Tip-jet gyroplane	Hover, Axial	Tip-driven rotor
	Cruise	Autogyro, Wing, Prop
	Conversion	Tip-driven rotor Wing, Prop

2.3.1. Hovering, Axial Flight Analysis

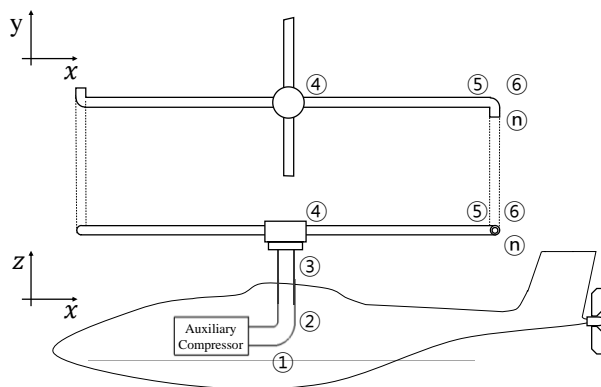


Figure 6: Internal Duct System

The inner duct system for the tip-jet is depicted in Fig. 6. The compressed gas from the auxiliary compressor flows from point ①~⑥ and is expelled from the nozzle creating a reaction force to drive the main rotor. To analyze the hover and axial flight, the analysis flow chart is depicted on Fig. 7. By using 1) ~ 3) steps, this analysis module obtains the following outputs: the rotational speed of the rotor, the nozzle contraction ratio, and the required power. 1) Analysis of the main rotor is performed using the BEMT, like the winged helicopter main rotor analysis, calculating the rotation speed and the required power. 2) The slip stream velocity is used to calculate the additional vertical drag of the fuselage and the wing caused by the rotor wake. 3) The contraction ratio of the nozzle that satisfies the required power and the rotation speed is calculated by the duct flow analysis. To account for the duct pressure loss, adiabatic condition is assumed. In addition, using the Fanno line theory equation (11), one-dimensional analysis was carried out [11]. Also, the pressure loss of the bent duct was considered using equation (12), and the loss factor K used in this study was based on the reference [12]. Equation (13) and (14) were used to calculate the

reaction force. The required power at the nozzle exit and the nozzle contraction ratio, which satisfies the required power calculated from the rotor aerodynamic analysis, were derived.

$$(11) \frac{dM}{dr} = \frac{M \left(1 + \frac{\gamma-1}{2} M^2\right)}{1 - M^2} \left(\frac{\gamma M^2}{2} \left(\frac{4f}{d}\right) - \frac{\Omega^2 r}{R_{gas} T} \right)$$

$$(12) P_{t2} = P_{t1} - Kq_{\infty}$$

$$(13) F_N = \dot{m}V_{jet} + A_N(P_N - P_{\infty})$$

$$(14) P_{avail} = P_{F_N} - P_{co} = N_b F_N (\Omega R_r) - N_b \dot{m} (\Omega R_r)^2$$

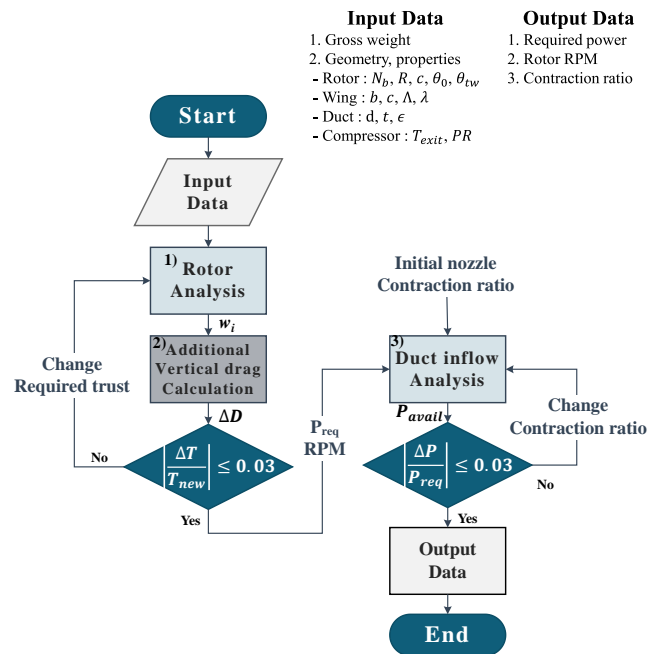


Figure 7: Hovering, Axial Flight Analysis Flow Chart (Tip-Jet)

2.3.2. Conversion Flight Analysis (Tip-Jet)

The conversion flight refers to the mode flying with a tip driven rotor, wing, and propeller. In this study, it was mainly used in the transient flight analysis of the tip-jet gyroplane. The conversion flight analysis flowchart is shown in Fig. 8. By utilizing 1) ~ 4) processes, it calculates the required power, the rotor rotational speed, the nozzle contraction ratio and the lift sharing factor. 1) The wing analysis is performed with the input gross weight and geometry shape parameters. 2) Aerodynamic analysis of the main rotor producing lift equivalent to the derived lift sharing factor is carried out. Since the rotor wakes would generate additional drag force on the fuselage and the wing, these vertical forces are calculated in the same manner as the winged helicopter. 3) The aerodynamic analysis of the auxiliary propeller thrusting the total drag force of the aircraft is carried out. 4) Assuming a fixed transmission loss, the required power is calculated for the conversion mission.

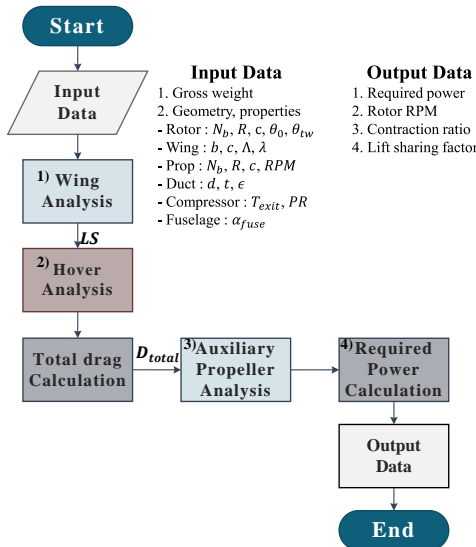


Figure 8: Conversion Flight Analysis Flow Chart (Tip-Jet)

2.3.3. Cruise Analysis

The tip-jet gyroplane cruise analysis flowchart is shown in Fig. 9, and it calculates the required power, rotor rotational speed, shaft tilt angle, and the lift sharing factor by using 1) ~ 3) steps. 1) The wing analysis, like the winged helicopter, is performed with the input gross weight and geometry shape parameters. 2) Aerodynamic analysis of the main rotor producing lift equivalent to the derived lift sharing factor is carried out. In addition, utilizing the equation (15), the rotor rotational speed and shaft tilt angle while satisfying the autogyro condition are calculated [13]. For this analysis, a linear twist assumption and uniform inflow model was applied similar to the winged helicopter. 3) As depicted in Fig. 10, the aerodynamic analysis of the auxiliary propeller thrusting the total drag force of the aircraft is carried out. 4) Assuming a fixed transmission loss, the required power is calculated for the cruise mission.

$$(15) P_{req} = P_0 + P_i - D_r V_\infty = 0$$

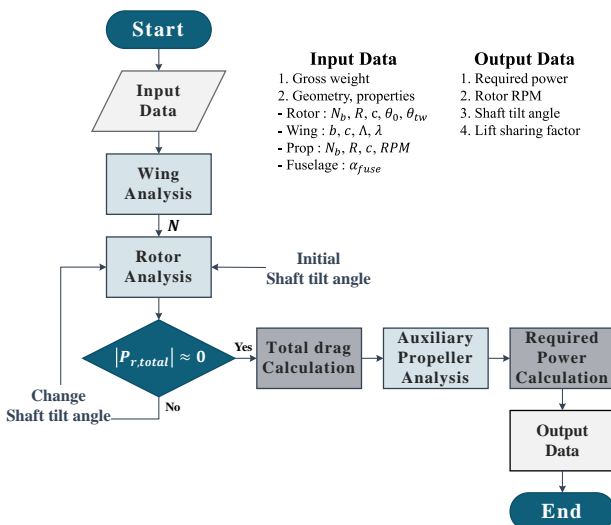


Figure 9: Cruise Analysis Flow Chart (Tip-Jet)

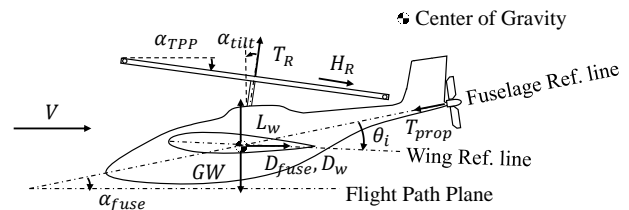


Figure 10: Acting Forces at Cruise (Tip-Jet)

2.4. Mission Analysis : Fan-in-body

Fan-in-body is considered a compound helicopter that combines ducted fan and wing. The flight performance is shown in Table 4. The fan-in-body concept uses the fan to perform hover and axial flight, and during forward flight, the wing produces lift to perform like a fixed-wing aircraft.

Table 4: Flight Performance of Fan-in-body

	Flight condition	Force generation
Fan-in-body	Hover, Axial	Fan, Prop
	Cruise	Wing, Prop
	Conversion	Fan, Wing, Prop

2.4.1. Hovering and Axial Flight Analysis (FIB)

As depicted in Fig. 11, fan-in-body concept not only produces lift from the fan but also from the duct itself. This additional drag is accounted during hover and axial flight analysis to compute the required power. Flowchart of hover and axial flight analyses are represented in Fig. 12. By using 1) ~ 3) steps, this analysis module obtains the following output: required power. 1) Thrust due to the duct is computed using the input parameters such as the initial gross weight and various duct design variables. 2) Using the equation (16), total thrust generated by the duct and the fan is computed [14]. 3) The total power required to perform the hover and axial flight considering the shroud effect and the power loss by the transmission is calculated. With the equation (17), additional power required due to the vane was assumed to be a fixed 6% of the required power [15].

$$(16) T_{fan} = \frac{T_{total}}{2\sigma_d}, \quad \sigma_d = \frac{A_{fan}}{A_{duct}}$$

$$(17) P_{fan} = 1.06 \left[\kappa_{fan} \frac{T_{total}^{1.5}}{\sqrt{4\rho A \sigma_d}} + \frac{C_{d0} \sigma_{fan}}{8} \rho A V_{tip}^3 \right]$$

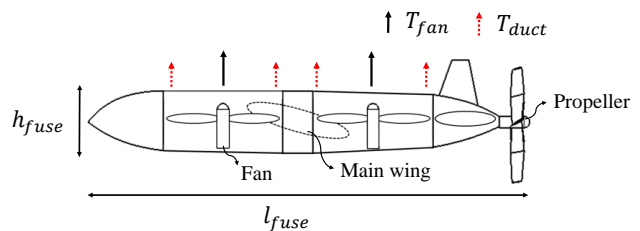


Figure 11: Fan-In-Body Configuration

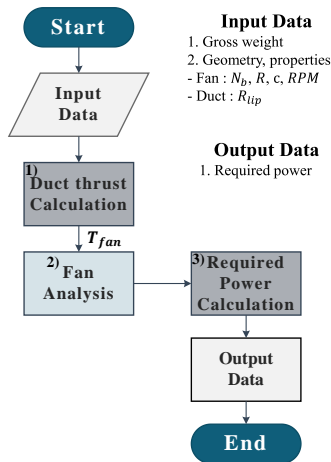


Figure 12: Hovering, Axial Flight Analysis Flow Chart (FIB)

2.4.2. Conversion Flight Analysis

Conversion flight analyzes the fan, wing, and the propeller which is used to compute the transient performance of the fan-in-body concept. The flowchart is depicted in Fig. 13, and this module computes the power required and the fuselage angle essential to analyze the mission during the conversion flight analysis through 1) ~ 4) steps. 1) The wing analysis is performed with the input gross weight and geometry shape parameters. 2) An aerodynamic analysis of the fan producing lift equivalent to the derived lift sharing factor is carried out. With the equation (18) and (19), Additional drag and power loss due to the duct during forward flight are modeled [16][17]. 3) Summing up all the power required and power losses due to various components such as the transmission and the duct, overall power required for the conversion flight analysis is computed.

$$(18) D_{fan} = -\frac{\sigma_d \rho A w_i}{\sqrt{\cos \alpha}} (V_\infty - w_i \sqrt{\cos \alpha} \tan \alpha)$$

$$(19) P_{fan} = P_{fan,1} + 1.13P_{fan,2} + \dots + 1.13P_{fan,n}$$

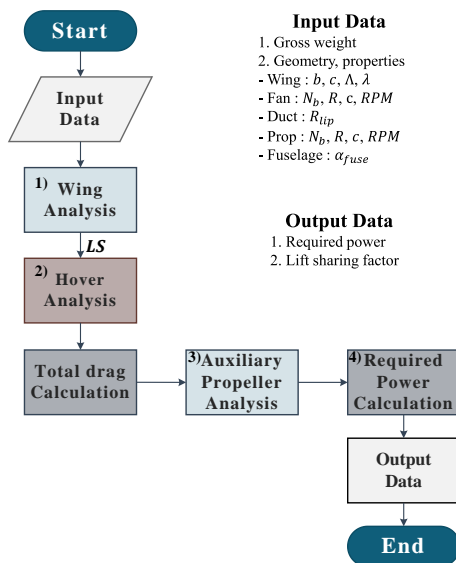


Figure 13: Conversion Flight Analysis Flow Chart (FIB)

2.4.3. Cruise Analysis (FIB)

Since the fan-in-body concept closes the fan and performs forward maneuver in the form of fixed-wing aircraft, similar fixed-wing cruise analysis is performed. Flowchart of the mission analysis is illustrated in Fig. 14. Through 1) ~ 3) procedures this analysis module obtains the following outputs: the propeller aerodynamic performance and the fuselage angle. 1) The wing analysis is performed with the input gross weight and geometry shape parameters. 2) An aerodynamic analysis is performed on the auxiliary propeller bearing the total drag force of the aircraft, and the fuselage angle is computed by iterative calculation. For this analysis, k_{prop} is set to 1. 3) The total required power by the wing, fuselage, and the propeller, accounting for the transmission loss, is calculated.

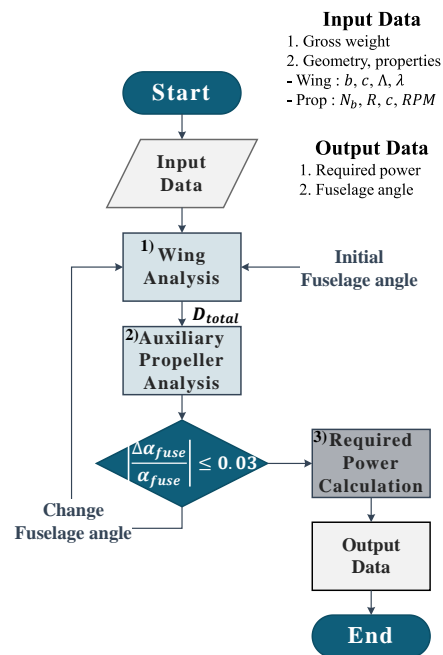


Figure 14: Cruise Analysis Flow Chart (FIB)

3. DESIGN OPTIMIZATION RESULTS

Various concepts of compound helicopters have been suggested. Each concept has different aerodynamic characteristics and propulsion system according to the configurations. In view of their unique feature, each concept is adapted with a specific mission profile. In order to suggest the appropriate concept for a specific mission, the design optimizations were conducted for six mission profiles covering various flight range, hover and loiter time. The standard mission profile consists of outbound cruise, hover, loiter, and inbound cruise respectively as shown Fig. 15. The standard mission range is 200 nm, which is the maximum straight-line distance in South Korea. Based on the standard mission, remaining five mission profiles are shown in Table 5.

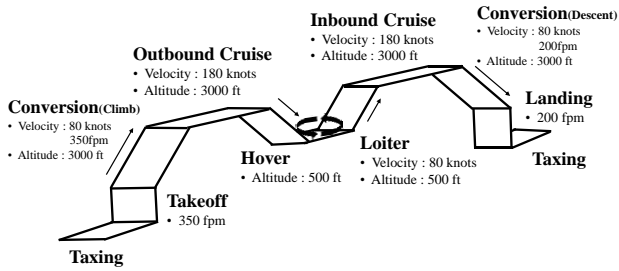


Figure 15: Standard Mission Profile (Case 1)

Table 5: Specification of Mission Profiles

	Mission Range [nm]	Hover / Loiter time [min]	Total Endurance [min]
Case 1 (Standard)	200	15 / 15	217
Case 2	300	15 / 15	284
Case 3	400	15 / 15	350
Case 4	200	30 / 30	247
Case 5	200	45 / 45	277
Case 6	200	60 / 60	307

3.1. Design Assumptions

Detailed requirements for design were replaced by several assumptions at the conceptual design phase. The applied assumptions are as follows.

1) Winged helicopter

- 1-1) It has an articulated rotor, and shaft axis is located at the C.G point of the aircraft.
- 1-2) Based on the actual helicopter characteristics, fuselage's width and height are assumed to be $0.3R_{mr}$, and the length from the landing gear to hub is $0.6R_{mr}$ [18].
- 1-3) It drives the rotor and propeller utilizing two identical engines. The complicated transmission mechanism to connect the engine to the rotor and the propeller, were estimated by adding an extra of 10% to the weight of the transmission per engine.
- 1-4) It reduces the speed of the rotor when performing a high speed flight above a specific speed. This study assumes that the reference speed for decelerated rotor is 100 knots. Also, the weight of the transmission capable of slowing down the rotor is estimated based on the reduced rotational speed of rotor.

2) Tip-jet gyroplane

- 2-1) It has a rigid rotor, and shaft axis is located at the C.G point of the aircraft.
- 2-2) Based on the actual helicopter characteristics, fuselage's width and height are assumed to be $0.3R_{mr}$, and the length from the landing gear to hub is $0.6R_{mr}$ [18].
- 2-3) It obtains the required power by the cold cycle utilizing the auxiliary compressor and turboshaft engine [19].
- 2-4) The weight of the auxiliary compressor is estimated

to be 20% of the total weight of the main engine [20].

- 2-5) The material of the inner duct is stainless steel.
- 2-6) A circular duct is used from the compressor to the hub, and an elliptical duct is equipped within the rotor.
- 2-6) Pressure loss coefficient of the bent portions of the duct are between 0.4 to 0.5 [12]

3) Fan-in-body

- 3-1) The distance between the ducted fans is $0.5R_{fan}$ [21].
- 3-2) To have the space of ducted fan, the fuselage's width is assumed to be $1.1d_{fan}$ and length is $3.5d_{fan}$ [16]. Based on the characteristics of Phantom swift, fuselage height is $0.3w_{fuse}$.
- 3-3) In forward flight, fuselage generates the lift sized 10% of the lift occurred at the wing [22].
- 3-3) It drives the rotor and propeller utilizing two identical engines. The complicated transmission mechanism to connect the engine to the rotor and the propeller, were estimated by adding an extra of 10% to the weight of the transmission per engine.
- 3-4) The material of the duct is carbon-fiber composite [14].
- 3-5) Additional power required due to the vane was assumed to be a fixed 6% of the required power [15].

3.2. Problem Definition

TOGW is one of the vital parameter when comparing the performance of the aircraft with the same mission profile. Therefore, single objective optimization problem to minimize TOGW was carried out with two performance constraints and five geometrical constraints. Performance constraints consist of V_{max} and M_{tip} . To perform the given mission profile safely, maximum cruise speed is restricted to be larger than 110% of the cruise speed. In addition, to prevent the drag divergence from occurring, tip Mach number is limited to be under 0.85. Furthermore, rotor's aspect ratio is constraint to account for the structural instability of the rotor. Based on the Eurocopter X³ rotor, maximum aspect ratio of the rotor was set to 16. The constraint for the wing maximum angle of attack was to be 16°, which is the stall angle of the NACA2412 airfoil. For the realistic design of the auxiliary propeller, it was sized with the ground clearance consideration, $0.3R_r$. The maximum wing span was set to be $1.34l_{fuse}$ to account for the overall dimension of the aircraft, and based on the developed compound helicopters' dimensions, the wing was positioned between 0.3 to 0.5 l_{fuse} .

Objective (1):

$$\text{Min. Take-Off Gross Weight (lb), TOGW}$$

Constraints (7):

$$\begin{aligned} 1.1 V_{cruise} &\leq V_{max} & M_{tip,r} &\leq M_{dd} \\ AR_r &\leq AR_{limit} & \alpha_{eff,w} &\leq \alpha_{stall} \\ b_w &\leq b_{limit} & R_{prop} &\leq R_{limit} \\ l_{w,min} &\leq l_w & &\leq l_{w,max} \end{aligned}$$

Design variables consist of parameters concerning the rotor/fan, wing, propeller, duct etc. The baseline characteristics of each concept were used to define the design space, and the baselines used were the X3, the Rotodyne, and the Emperor [2][22][23]. Design parameters and spaces were described in Table A1 and A2.

Table 6: Design Variables for Compound Helicopters

Concept	Type	Variables
Winged helicopter (14)	Rotor	R, c, V_{tip}, SR
	Wing	$LS, AR, \lambda, \theta_{incid}$
	Prop	R, c, RPM, TR
	HT tail	b, AR
Tip-jet gyroplane (16)	Rotor	$R, c, \theta_0, \theta_{tw}$
	Wing	$LS, AR, \lambda, \theta_{incid}$
	Prop	R, c, RPM
	HT tail	b, AR
	Etc.	D_1, T_{exit}, PR
Fan-in-body (15)	Fan	N_b, R, c, V_{tip}
	Wing	$WL, AR, \lambda, \theta_{incid}$
	Prop	R, c, RPM
	HT tail	b, AR

3.3. Optimization Results (Standard : Case1)

Since most of the analysis equation in this study are made up of algebraic equations, the calculation time is approximately 5 to 10 seconds per case. Using this advantage of short computational time, the optimal design was performed by utilizing the non-gradient based method, Evolutionary optimization method. Despite designing the compound helicopters performing the same mission, different optimal design results were derived for each concept as shown in Table 9 and A3.

3D modeling of design results was shown in Fig. 16. Tip-jet gyroplane had a rotor radius smaller than the winged helicopter. However, chord of the tip-jet gyroplane, required to account for the internal duct in the rotor, was designed larger than rotor of the winged helicopter. Also, propellers of all concepts were designed to be the largest size satisfying the geometry constraint; ground clearance. For fan-in-body concept, it had the largest wing among all three concepts for the way to generate the sufficient lift during forward flight. Each concept had different TOGW as

Table 7: Results of Depsign Optimization (Standard)

	Winged helicopter	Tip-jet gyroplane	Fan-in-body
Take-off gross weight [lb]	2844	2770	2846
Empty weight [lb]	1504	1379	1686
Fuel weight [lb]	739	788	558
Maximum power [HP]	662 @ Cruise 200 knots	647 @ Cruise 200 knots	831 @ Transient 24 knots

well as different geometry. These different design results derived from each concept can be summarized into two main reasons. Firstly, different components in each aircraft results a difference empty weight. Fig. 17 represents the weight fraction for each concept. Winged helicopter structure had the lowest empty weight portion among all three concepts, being 32%, whereas its propulsion group being the highest portion, 54%, of the empty weight. The Winged helicopter rotor is an articulated rotor, and the aspect ratio was designed within the boundary of the aforementioned constraint given. With this, rotor weight was predicted to be 22% lighter than tip-jet gyroplane using a rigid rotor and an aspect ratio of 11. Furthermore, since the wing of the winged helicopter is also designed to be the smallest of all three concepts, the ratio of the winged helicopter structure group was calculated to be the smallest. However, largest transmission was sized for the winged helicopter to equip with two types of transmissions for the rotor and propeller, and the total transmission weight turn out to be 250 lb. Tip-jet gyroplane requires a rigid rotor, internal ducts, and auxiliary compressors for the tip-jet system, but do not require a transmission to drive the rotor. Therefore, the empty weight of tip-jet gyroplane was about 38% for structural group and 44% for propulsion group. Finally, when comparing the maximum required power, fan-in-body concept required the highest 831HP which is required for the additional drag during transient flight. Therefore, the fan-in-body concept had the heaviest engine designed at 564lb.

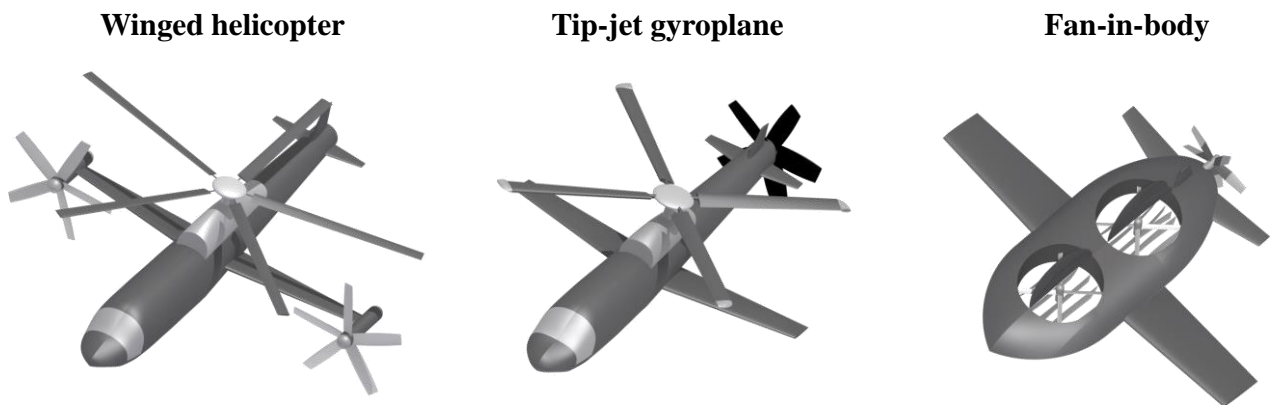


Figure 16: 3D Modeling of Design Optimization Results (Standard)

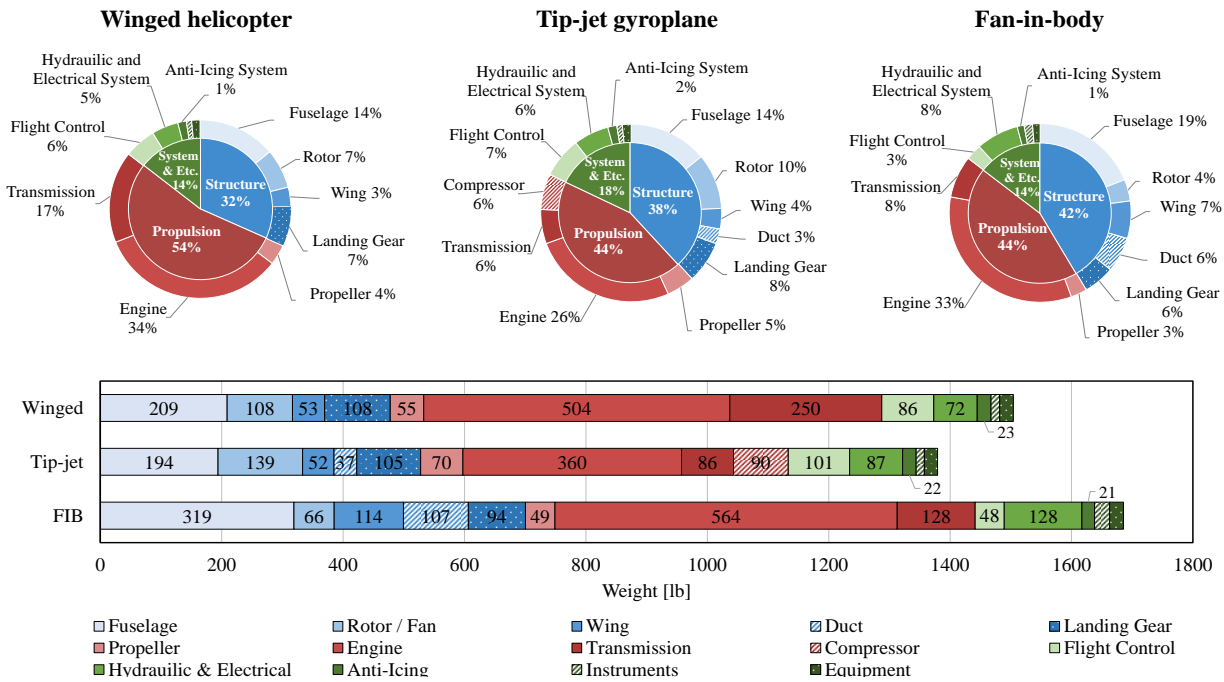


Figure 17: Weight Fractions of Compound Helicopters (Standard)

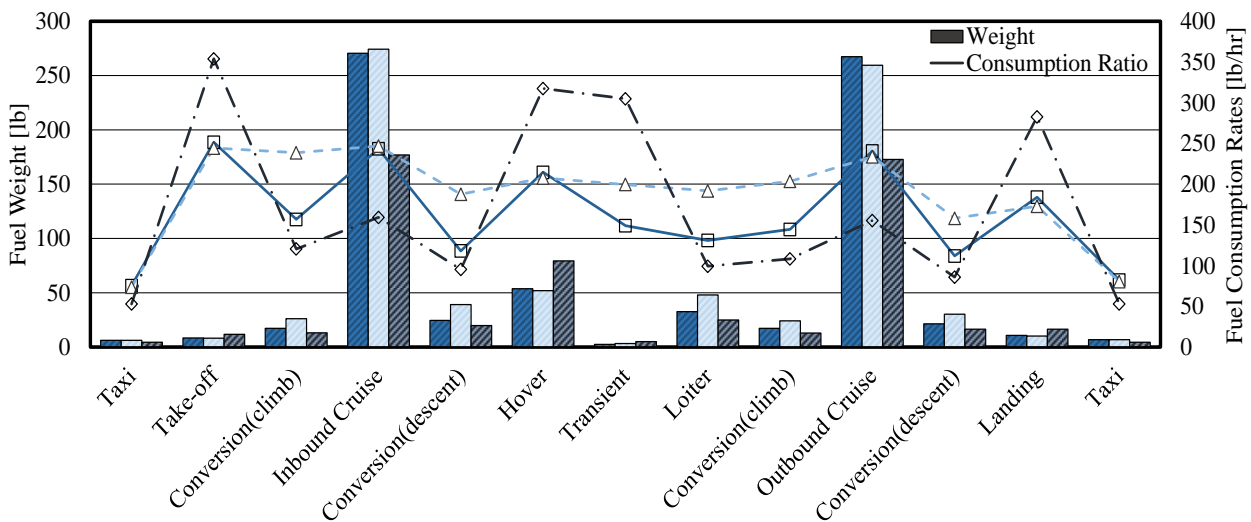


Figure 18: Fuel Weight and Consumption Rates at Mission Segments (Standard)

The second factor is due to the difference in the way each concept performs its mission, which results in a difference in the fuel consumption rate and the total fuel weight. Fig. 18 represents the amount of fuel and the fuel consumption for each mission segments. Through this, winged helicopter had the highest fuel consumption during take-off, hover, landing and cruise segments. When performing hover and axial flight, winged helicopter requires additional power to offset the anti-torque generated by the rotor, which accounts for 15% of the total power. Therefore, during hover and axial flight, the required power was higher than the tip-jet gyroplane. However, when performing the conversion mission, the winged helicopter controls the yawing moment using rudder and thereby power to counteract the anti-torque is almost negligible. Therefore, it consumed less fuel during forward flight when compared to the hover and axial flight. The tip-jet

gyroplane calculated a similar fuel consumption rate when performing the missions except for the cruise mission. While performing low speed flight at 80knots, the lift generated by the wing is insufficient, producing about 15% of the total lift. This led to the tip-jet requiring similar required power for most of the mission segment except for the cruise. The fan-in-body concept, on the other hand, required significantly less fuel when cruising compared to other concepts, with a difference of up to 35%. This is due to the fact that the fan-in-body concept performs the mission much more efficiently than the two other concepts, because it closes the fan and flies in the form of a fixed wing aircraft during forward flight. In hover and axial flight, however, a fan was used to generate lift, and this required power was 49% higher than other concepts. Upon reaching the required speed for the wing to generate 100% lift, it travels in the form of a fixed-wing aircraft.

Therefore, when performing the conversion mission, it travels in the form of fixed wing. Hence, fan-in-body required the least fuel consumption rate and fuel among the three concepts.

The prominent difference in the design results of each concept were mainly due to the listed two factors. In order to compare the results of the compound helicopter design, optimal design was additionally performed by varying the mission radius or by varying the hover and loiter time and will be described in section 3.4.

3.4. Optimization Results (Variation : Case2-6)

In order to derive the mission profile suitable for each of the three types of compound helicopter concept, the optimal design was performed by varying the mission radius or hover and loiter time based on the standard mission baseline. This results are shown in Table A3 ~ A5. Fig. 19 shows the aircraft TOGW when the mission range increases up to 400nm based on the standard mission. Since the fan-in-body concept performs forward flight in the form of a fixed-wing aircraft, the required power in forward flight is significantly smaller than other concepts. An increase in mission range means that the percentile of the forward flight for the entire mission is increased. Therefore, the TOGW difference between the fan-in-body concept and other two concepts took up to 13% when the mission range increases 200nm to 400nm. This shows that the fan-in-body concept is more appropriate concept when performing long-range missions. However, when hover and loiter time were increased, the opposite results were obtained as illustrated in Fig. 20. The fan-in-body concept uses the ducted fans to perform hovering, the fan requires 72% additional power than the other concepts. Subsequently, the amount required fuel also increases as the hover time was increased, the maximum TOGW difference between the other concepts was up to 16%. Therefore, winged helicopter and tip-jet gyroplane are seemingly the desirable concepts when carrying out short-range mission with prolonged hover and loiter mission.

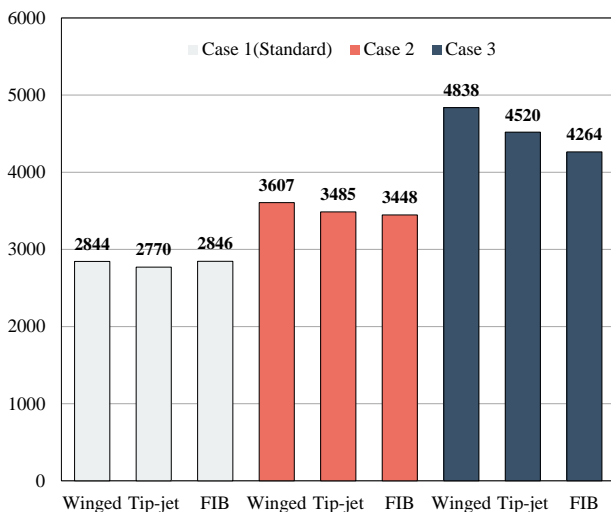


Figure 18: Result of Design Optimization (Mission Range)

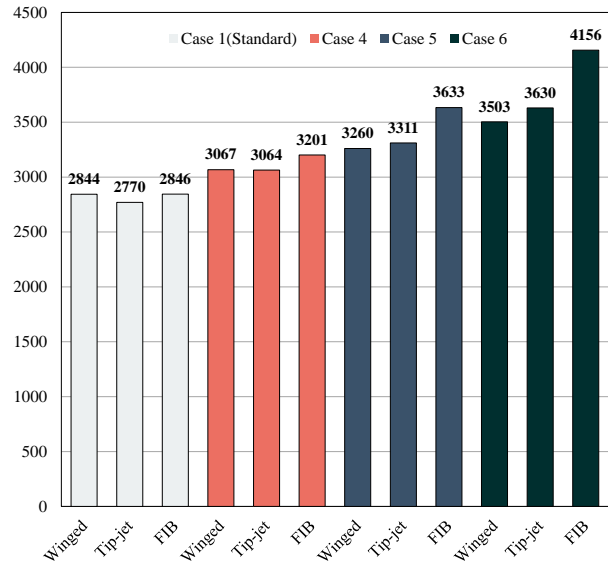


Figure 20: Result of Design Optimization (Hovering & Loiter Time)

4. CONCLUSION

This study developed a comprehensive conceptual design tool for the three concepts, winged helicopter, tip-jet gyroplane, and fan-in-body concept. This design tool has the comparable analysis fidelity, while considering their distinctive propulsion system at the conceptual design phase. Utilizing the developed tool, the design optimizations were conducted for six different mission profile covering various flight range, hover and loiter time. As a result of the design optimizations, the following conclusions were drawn:

- 1) Fan-in-body concept is more appropriate concept when performing long-range missions. Since the fan-in-body concept carries out the cruise mission in the form of a fixed-wing aircraft, the required power in the cruise mission is noticeably smaller than other concepts. In addition, the TOGW difference between the fan-in-body concept and other two concepts was 13% at 400nm.
- 2) On the other hand, since the fan-in-body concept uses the ducted fans to perform hovering, the winged helicopter and the tip-jet gyroplane are seemingly the desirable concepts when carrying out short-range mission with prolonged hover and loiter mission. Also, the TOGW difference between the fan-in-body and other concepts was calculated up to 16%.

In the aircraft design, not only aerodynamic analysis but also noise and structural stability analysis are important factors. In the future, if the multidisciplinary design considering noise and structural stability are carried out utilizing the concept design tool of this study, it will be possible to compare various compound helicopters from a more realistic point of view.

ACKNOWLEDGEMENT

This research was conducted at High-Speed Compound Unmanned Rotorcraft (HCUR) research laboratory with the support of Agency for Defense Development (ADD).

REFERENCE

- [1] Hwang, C. J., and Kim, S. B., "Analysis and Trend Curve Derivation of Major Design Parameters of Unmanned and Manned Rotorcrafts," Journal of The Korean Society for Aeronautical and Space Sciences, Vol. 34, No. 2, 2006, pp. 26~35.
- [2] Roche, J., "Aerodynamic Trade Study of Compound Helicopter Concepts," Embry-Riddle Aeronautical University, Master of Science in Aerospace Engineering, 2015.
- [3] Vu, N. A., Lee, Y. J., Lee, J. W., Kim, S. H., Chung, I. J., "Configuration Design and Optimisation Study of a Compound Gyroplane," Aircraft Engineering and Aerospace Technology, Vol. 83, No. 6, 2011, pp.420~428
- [4] Lee, H., Prasad, R. and Choi, S., "Aerodynamic Analysis for Conceptual Design of a Lift-Fan Type Aircraft", AIAA Aviation 2016, Washington, D.C., July 2016.
- [5] Kim, W. J., Chae, S. H., Oh, S. J., Kim, S. B., Ahn, L. K., Yee, K. J., "Systematic Determination of Empirical Parameters Used in Helicopter Conceptual Design," Journal of The Korean Society for Aeronautical and Space Sciences, Vol. 44, No. 8, 2012, pp.703~710.
- [6] Schwartzberg, M. A., Smith, R. L., Means, J. L., Law, H. Y. H., and Chappell, D. P., "Single-Rotor Helicopter Design and Performance Estimation Programs, Volume 1, Methodology," U.S. Army Air Mobility R&D Laboratory, SRIO Report Number 77-1, 1977.
- [7] Leishman, J. G., Principles of Helicopter Aerodynamics, 2nd Ed, Cambridge University Press, Cambridge, New York, 2006.
- [8] Keys, C. N., "Rotary-Wing Aerodynamics Volume 2: Performance Prediction of Helicopters," NASA CR-3083, 1979, pp.143~153.
- [9] Nita, M., Scholz, D., "Estimating the Oswald Factor from Basic Aircraft Geometrical Parameters," Proceeding of the Deutscher Luft-und Raumfahrtkongress, August 2012.
- [10] Gessow, A., G. C. Myers, Jr., "Aerodynamics of the Helicopter," 3rd Ed, Frederick Ungar Publishing Company, 1967.
- [11] Jun, Y. M., Jung, Y. W., Yang, S. S., "Conceptual Design For a SUAV Propulsion System Sizing," Proceedings of the 24th International Council of the Aeronautical Sciences Congress, August 2004.
- [12] Jung, Y. W., Jun, Y. M., Yang, S. S., "The Application of CFD for the Duct System Design of CRW aircraft," Proceeding of the Korean Society of Computational Fluids Engineering Spring Conference, August 2003, pp.200~205.
- [13] Harris, F. D., "An Overview of Autogyros and The McDonnell XV-1 Convertiplane," NASA CR-2003-212799, 2003.
- [14] Pereira, J., "Hover and Wind-Tunnel Testing of Shrouded Rotors for Improved Micro Air Vehicle Design," Ph.D. Thesis, University of Maryland, College Park, MD, 2008.
- [15] Woodrow, L. C., "Summary of Lift and Lift/Cruise Fan Powered Lift concept Technology", NASA-CR-177619, 1993.
- [16] Roh, N. H., Oh, S. J., Park, D. H., "Numerical Investigation of Forward Flight Characteristics of Multi-Ducted Fan," Journal of The Korean Society for Aeronautical and Space Sciences, Vol. 46, No. 2, 2018, pp. 95~105.
- [17] Jang, J. S., Choi, I., Hyun, Y. O., Yim, J. B., "Preliminary Sizing of a Fan-in-Body Compound Rotorcraft," In the proceeding of the Korean Society for Aeronautical and Space Sciences Conference, November 2015, pp.861-864.
- [18] Prouty, R. W., "Helicopter Performance, Stability, and Control," PWS Publishers, 1986.
- [19] Taylor, J. W., Jane's pocket book of research and experimental aircraft, MacDonald and Jane's Publishers Ltd, 1976.
- [20] Gibson, A., Hall, D., Waters, M., Masson, P., Schiltgen, B., Foster, T., and Keith, J., "The Potential and Challenge of Turbo Electric Propulsion for Subsonic Transport Aircraft," 48th AIAA Aerospace Sciences Meeting Including the New Horizons Forum and Aerospace Exposition, April. 2010
- [21] Arkhipov, M., Serokhvostov, S., Stremousov, K., "Numerical and Experimental Investigation of Ducted Fans Interference for Multirotor Copter-type Aerial Vehicle," 7th European Conference for Aeronautics and Aerospace Sciences, Milan, July 2017.
- [22] Gibbings, D., "The Fairey Rotodyne — technology before its time?," The Aeronautical Journal, Vol. 108, No. 1089, 2004, pp. 565~574.
- [23] Jacobellis, G., Angilella, A., Reddinger, J., Howard, A., Misirowski, M., Pontecorvo, M., Krishnamurthi, J., "Emperior UAV, X-VTOL," 31st Annual American Helicopter Society Student Design Competition, 2014.
- [24] Sadraey, M. H., Aircraft Design: A Systems Engineering Approach, John Wiley & Sons, Chichester, West Sussex, 2012.
- [25] Johnson, W., "NDARC - NASA Design and Analysis of Rotorcraft," NASA/TP-2015-218751, 2015.
- [26] Raymer, D. P., Aircraft Design: A Conceptual Approach, Education Series, AIAA, Washington, DC, 1992

APPENDIX

Main Wing Position Calculation

Using the equation (A1) and (A2), main wing position satisfying the static margin was calculated with the given center of gravity position [24]. Since the shaft axis of the rotor is located at the center of gravity, it was ignored when calculating the static margin.

$$(A1) \quad l_n = \text{Static Margin} - l_{c.g} = l_{ac} + \frac{l_h S_t}{c_w S_w} \frac{C_{L_{\alpha t}}}{C_{L_{\alpha, WB}}} \left(1 - \frac{\partial \epsilon}{\partial \alpha}\right)$$

$$(A2) \quad l_w = l_{fuse} - l_h$$

Empty Weight Estimation

Based on the reference [6], [25], and [26], the components weight estimation were carried out. In addition, the engine weight estimation was conducted utilizing the published engine data of EASA.

Structure group

1) Fuselage (Winged, Tip-jet)

$$W = 0.0265 TOGW^{0.943} R_r^{0.654} \text{ for Winged, Tip-jet}$$

$$W = 0.052 q_{\infty}^{0.241} S_{fuse}^{1.086} (1.5 TOGW)^{0.177} l_t \left(\frac{h_{fuse}}{l_{fuse}} \right)^{0.072} + W_{press} \text{ for FIB}$$

2) Main Rotor

$$W = W_b + W_{hub} + W_{spin} \text{ for articulated rotor}$$

$$W = \kappa_{type} (W_b + W_{hub} + W_{spin}), \kappa_{type} = \frac{0.94 N_b c_r R_r^{1.75}}{1.54 N_b c_r R_r^{1.5}}$$

for rigid rotor

$$W_{blade} = 0.02606 N_b^{0.6592} R_r^{1.3371} c_r^{0.9959} V_{tip,r}^{0.6682} v_r^{0.5505}$$

$$W_{hub} = 0.00372 N_b^{0.281} R_r^{1.538} V_{tip,r}^{0.429} v_{hub}^{2.1414} (W_{blade})^{0.551}$$

$$W_{spin} = 7.386 (0.05 R_r)^2$$

3) Fan

$$W = 9.035 N_{fan} N_b^{-0.486} RPM_{fan}^{-0.459} d_{fan}^{0.157} \left(\frac{P_{max,fan}}{N_{fan}} \right)^{0.92}$$

4) Main wing

$$W = 0.036 S_w^{0.758} \lambda_w^{0.04} (1.5 TOGW)^{0.49} \left(\frac{AR_w}{\cos^2(\Lambda_w)} \right)^{0.6} \times \left(\frac{100}{\cos(\Lambda_w)} \frac{t}{c} \right)^{-0.3}$$

Horizontal tail wing

$$W = 0.7176 S_{HT} AR_{HT}^{0.3173}$$

Vertical tail wing

$$W = 1.046 S_{VT} AR_{VT}^{0.5332}$$

5) Duct

$$W = \rho_{duct} N_{duct} V_{duct}$$

6) Landing gear

$$W = 0.038 TOGW$$

Propulsion group

1) Propeller

$$W = 9.035 N_{prop} N_b^{-0.486} RPM_{prop}^{-0.459} d_{prop}^{0.157} \left(\frac{P_{max,prop}}{N_{prop}} \right)^{0.92}$$

2) Engine

$$W = W_{dry eng} + W_{accessories} + W_{exhaust}$$

$$W_{dry eng} = 9.227 N_{eng} P_{max}^{0.5365} \left(\frac{TOGW}{N_{eng}} \right)^{-0.01035}$$

$$W_{accessories} = 2.973 N_{eng}^{0.7858} \left(\frac{W_{dry}}{N_{eng}} \right)^{0.5919}$$

$$W_{exhaust} = N_{eng} (0.006 P_{max})$$

3) Transmission

$$W = 196 \left(\frac{P_{xmsn,limit}}{RPM} \right)^{0.858}$$

4) Auxiliary compressor

$$W = 0.25 W_{eng}$$

System & Etc. group

1) Flight control

$$W = 0.5045 c_r^{0.659} (TOGW)^{0.689} \text{ for Winged, Tip-jet}$$

$$W = 0.0168 TOGW \text{ for FIB}$$

2) Hydraulic & Electrical system

$$W = 0.1905 R_r (P_{max})^{0.616} \text{ for Winged, Tip-jet}$$

$$W = 0.045 TOGW \text{ for FIB}$$

3) Anti-Icing

$$W = 0.008 TOGW$$

4) Instruments

$$W = 0.000385 (TOGW)^{1.321}$$

5) Equipment

$$W = 0.00074 (TOGW)^{1.298}$$

Design Parameters and Variables

Table A1: Design Parameters of Compound Helicopters

Design parameters		Value
Rotor / Fan	Airfoil	Winged : NACA 0012 Tip-jet : NACA 0018 FIB : NACA 0012
	N_b	Winged : 5 Tip-jet : 4 FIB : 4
	Wing	Winged : NACA 2412 Tip-jet : NACA 2412 FIB : NACA 23012
H-tail wing	ϕ	15
	Airfoil	NACA 2412
V-tail wing	λ	0.4
	Λ [deg]	15
	Airfoil	NACA 2412
	b [ft]	1.99
H-tail wing	AR	1.5
	λ	0.4
	Λ [deg]	20

	Engine	GE-T700
	PR	5
Etc.	T_{exit} [°R]	1000
	t_{duct} [%]	0.1
	Design Payload [lb]	600

Table A2: Design Variables of Compound Helicopters

Concept	D.V	Design space
Winged helicopter	R_r	$6.3 \leq R_r \leq 17.0$
	c_r	$0.39 \leq c_r \leq 1.07$
	$V_{tip,r}$	$403 \leq V_{tip,r} \leq 940$
	SR	$0.51 \leq SR \leq 1.0$
	TD	$0.2 \leq TD \leq 1.0$
Tip-jet gyroplane	R_r	$7.5 \leq R_r \leq 21.1$
	c_r	$0.50 \leq c_r \leq 1.38$
	θ_0	$8.4 \leq \theta_0 \leq 16$
	D_{duct}	$0.3 \leq D_{duct} \leq 1.7$
	PR	$2.7 \leq PR \leq 6.3$
Fan in body	T_{exit}	$540 \leq T_{exit} \leq 1260$
	N_b	$2 \leq N_b \leq 4$
	R_{fan}	$1.87 \leq R_r \leq 4.35$
	c_{fan}	$0.33 \leq c_r \leq 0.77$
	$V_{tip,fan}$	$245 \leq V_{tip,fan} \leq 982$
Common	WL	$10 \leq WL \leq 47$
	θ_{tw}	$-13 \leq \theta_{tw} \leq -5$
	θ_{incid}	$2 \leq \theta_{incid} \leq 21$
	LS	$0.24 \leq LS \leq 1.0$
	AR_w	$2.84 \leq AR_w \leq 8.8$
	λ_w	$0.27 \leq \lambda_w \leq 1.0$
	R_{prop}	$2.76 \leq R_{prop} \leq 6.44$
	c_{prop}	$0.5 \leq c_{prop} \leq 1.5$
	RPM_{prop}	$500 \leq RPM_{prop} \leq 1800$
	TD	$0.2 \leq TD \leq 1.0$
b_t	$3.57 \leq b_t \leq 28.9$	
AR_t	$2.84 \leq AR_t \leq 7.7$	

Optimization Results

Table A3: Optimization Result of Winged Helicopter

D.V	Optimized values of 6 cases					
	1	2	3	4	5	6
R_r	9.42	9.93	11.7	9.87	9.43	9.83
c_r	0.59	0.64	0.78	0.62	0.60	0.62
$V_{tip,r}$	597	607	597	607	597	597
θ_{tw}	-11.	-8.0	-9.1	-9.0	-8.6	-10
SR	1.0	1.0	1.0	1.0	1.0	1.0
LS	0.57	0.49	0.51	0.64	0.55	0.60
θ_{incid}	15.0	17.9	16.4	16.6	18.4	19.6
AR_w	6.58	6.62	6.62	3.83	6.17	6.17
λ_w	0.41	0.41	0.33	0.44	0.38	0.46
R_{prop}	2.82	2.98	3.51	2.92	2.81	2.91
c_{prop}	0.50	0.50	0.52	0.52	0.50	0.50
RPM_{prop}	1800	1780	1494	1784	1800	1800
TD	0.80	0.79	0.80	0.78	0.77	0.73
b_t	3.57	3.57	3.57	3.57	3.57	3.57
AR_t	4.64	4.19	3.68	6.00	5.60	5.47

Table A4: Optimization Result of Tip-Jet Gyroplane

D.V	Optimized values of 6 cases					
	1	2	3	4	5	6
R_r	11.1	12.8	10.1	10.5	11.5	
c_r	0.80	0.87	0.79	0.82	0.85	
θ_0	16.0	16.0	15.8	16.0	15.8	
θ_{tw}	-8.2	-9.6	-8.5	-9.0	-6.3	
LS	0.29	0.36	0.31	0.36	0.29	
θ_{incid}	3.28	3.76	3.12	4.24	3.68	
AR_w	7.37	8.80	6.49	8.80	8.14	
λ_w	0.46	0.42	0.39	0.54	0.46	
R_{prop}	3.32	3.81	3.02	3.12	3.41	
c_{prop}	0.54	0.50	0.56	0.92	0.54	
RPM_{prop}	1754	1702	1598	1800	1702	
b_t	5.19	4.24	5.89	3.67	3.67	
AR_t	4.51	4.96	5.22	4.58	2.64	
D_{duct}	0.52	0.50	0.47	0.46	0.47	
PR	5.36	5.65	4.79	4.72	4.93	
T_{exit}	742	785	1096	1173	1015	

Table A.5: Optimization Result of Fan-In-Body

D.V	Optimized values of 6 cases					
	1	2	3	4	5	6
$N_{b,fan}$	2	2	2	2	2	2
R_{fan}	2.47	2.57	2.75	2.28	2.50	2.68
c_{fan}	0.28	0.30	0.32	0.27	0.30	0.32
$V_{tip,fan}$	942	942	942	942	942	942
WL	45.3	42.8	46.6	42.8	45.3	46.8
θ_{incid}	16	16	16	16	16	16
AR_w	7.6	6.8	7.5	6.8	7.2	6.9
λ_w	0.72	0.72	0.71	0.67	0.72	0.72
R_{prop}	2.54	2.64	2.84	2.34	2.54	2.73
c_{prop}	0.5	0.5	0.62	0.76	0.5	0.5
RPM_{prop}	1800	1800	1800	1800	1800	1800
b_t	8.43	11.3	11.3	10.3	9.7	12.2
AR_t	5.	6.9	7.6	7.5	6.3	7.7

Copyright Statement

The authors confirm that they, and/or their company or organization, hold copyright on all of the original material included in this paper. The authors also confirm that they have obtained permission, from the copyright holder of any third party material included in this paper, to publish it as part of their paper. The authors confirm that they give permission, or have obtained permission from the copyright holder of this paper, for the publication and distribution of this paper as part of the ERF proceedings or as individual offprints from the proceedings and for inclusion in a freely accessible web-based repository.